Conductivity and dielectric constant of nanotube/polymer composites

Yuichi Hazama,[1] Naoki Ainoya,[2] Jun Nakamura,[1,2,*] and Akiko Natori[1]
[1]*Department of Electronic-Engineering, The University of Electro-Communications (UEC-Tokyo), 1-5-1 Chofugaoka, Chofu, Tokyo 182-8585, Japan*
[2]*Department of Engineering Sciences, The University of Electro-Communications (UEC-Tokyo), 1-5-1 Chofugaoka, Chofu, Tokyo 182-8585, Japan*
(Received 1 May 2010; revised manuscript received 18 June 2010; published 16 July 2010)

The complex ac admittance of a thin film of carbon nanotube/polymer composites depending on both the concentration and the alignment of nanotubes has been studied. The complex ac admittance and the current intensity distribution is numerically calculated using a transfer matrix method, where the discretized mesh model for nanotube/polymer composites is transformed into the *RC* network. The percolation threshold increases with the degree of alignment of nanotubes. The vertical dc conductivity parallel to the alignment direction has the maximum at a specific alignment, which is caused by competition between the number of percolating paths and the degree of meandering of the current. Two extreme cases for the dc conductivity are studied; the nanotube-resistance (NT)-limited case and the contact-resistance (CR)-limited case. CR-limited conductivity has much stronger concentration dependence than NT-limited conductivity, since the number of parallel connections of contact-resistors increases more strongly with the nanotube concentration than that of nanotube resistors. The vertical static dielectric constant is enhanced near the percolation threshold and the enhancement is significantly enlarged with the alignment of nanotubes, due to both the decrease in the number of serial connections of minigap capacitors along the path of the imaginary current and the increase in the number of paths.

DOI: 10.1103/PhysRevB.82.045204 PACS number(s): 72.60.+g, 72.80.Tm, 61.43.Bn

I. INTRODUCTION

Recently, conductor-insulator composite materials such as metal-filled epoxy adhesives have been increasingly expected as a promising candidate to replace solder in microelectronics field. The properties of conductor-insulator composites have been extensively studied in both experimental and theoretical physics for many years.[1] One of the main theoretical models since 1970s has involved percolation theory and the concept of scaling.[2,3] Some powerful numerical methods to obtain the critical exponent near the percolation threshold have been developed, such as a transfer-matrix approach,[4] a position-space renormalization group[5] and efficient Monte Carlo algorithm.[6] Percolation theory has predicted a universal behavior of the electrical conductivity and the dielectric properties, which does not depend on details of the system but on the spatial dimension.

To reduce the percolation threshold, fine particles with a high-aspect ratio have been expected as the filler.[7] Indeed, carbon-nanotubes-filled polymeric materials have been shown as the conducting composite material with a very low-percolation threshold.[8–11] Homogeneous carbon nanotube/polymer composites were fabricated using noncovalently functionalized, soluble single-walled carbon nanotubes (SWNTs) and they showed dramatic improvement in the electrical conductivity with a very low percolation threshold (0.05–0.1 wt % of SWNT loading).[8] Homogeneous composites of SWNT/epoxy were also made by a high frequency sonication method.[9] The percolation threshold p_c was found to be 0.074 wt %. The electrically conductive carbon nanotube/polymer composites have various applications such as electromagnetic interference shielding and printable circuit wiring.[8]

Extensive experimental works have been performed for the dc conductivity, dielectric constant and the ac conductivity for carbon nanotube/polymer composites. Both alternating current (ac) and direct current (dc) conductivities have been measured for carbon nanotube/polymer thin films.[12] The ac conductivity displayed two distinct regions, a frequency-independent region at a lower frequency and a frequency-dependent region at a higher frequency. The dc conductivity σ followed a percolation scaling law of $\sigma = \sigma_0(p-p_c)^t$ with $t=1.36$ and the observed low value of σ_0 is attributed to charge transport controlled by fluctuation-induced tunneling between nanotubes. The scaling law of the dc conductivity holds in a surprisingly wide range of reduced volume fraction $(p-p_c)/p_c$, from 0.18 to 182 with $p_c = 0.055\%$. The similar scaling law with $t=1.54$ in a wide range was also observed for single-walled carbon nanotube/polystyrene composites, in a reduced mass fraction from 0.1 to 200.[8] Wang *et al.* studied the dielectric properties of the untreated multiwall carbon nanotube/poly vinylidene fluoride composites.[13] The low-frequency dielectric constant of a composite becomes as high as 300 near the percolation threshold and the value of dielectric loss is always less than 0.4 irrespective of the frequency in the insulating region. The composites with high-dielectric constant have an application to high-charge-storage capacitors. Giant dielectric constant near a percolation threshold has also been observed in carbon nanotube/rubber nanocomposites with low-percolation threshold.[14] At $p=0.012\%$, the dielectric constant is about 250 and it is over 1000 when the volume fraction is 0.015%. As for the dc conductivity, the best fits of the conductivity data to the log-log plots of the power law give $p_c = 0.012 \pm 0.001\%$ for the volume fraction and $t=2.85 \pm 0.15$, which is larger than the universal value of 2.0 in 3D.[1] Electrical properties of percolative carbon nanofiber/polystyrene

composites have also been studied and the scaling law with $t=1.3$ and $p_c=1.71\%$ for the volume fraction is observed.[15] The dielectric constant can also be expressed by the power law of $\varepsilon=\varepsilon_p|1-p/p_c|^{-s}$, where ε_p is the dielectric constant of the matrix. The experimental data are in good agreement with $p_c=1.71\%$ and $s=0.9$, and the dielectric constant over 200 is observed near the percolation threshold.

Percolation critical exponents for fine particles with a high aspect ratio were calculated theoretically, for the first time, in a two-dimensional (2D) system of randomly distributed conducting sticks.[16] It has been shown that the corresponding exponent, t, has the value of 1.24 ± 0.03 for the contact-resistance (CR)-limited conductivity. The authors claim that the exponent t has the same value for the nanotube-resistance (NT)-limited case within the "experimental" uncertainty. Here, CR-limited or NT-limited conductivity is determined by the contact resistance between nanotubes or the nanotube resistance, respectively. The geometric critical exponent β associated with the percolation probability, i.e., the probability that metallic fillers belong to the conducting network, was shown to have a value of 0.14 ± 0.02.[16] These results suggest that the 2D continuum system belongs to the same universality class as the 2D lattice system in which $t=1.3$ and $\beta=5/36=0.14$ are known.[1,17] Recently, Monte Carlo simulation on the effective electrical conductivity of short-fiber composites has been performed for the NT-limited case using randomly distributed three dimensional cylinders.[18] By discretizing the interconnected surfaces of individual fibers, a finite element method was applied to evaluate the equivalent electrical conductivity. Their result indicates that the dc conductivity increases monotonically with the decrease of the fiber orientation angle θ, defined as the angle between the fiber axis and the potential gradient. In their calculations, both the fiber number and the ratio of the fiber length to the simulation cell size are not sufficiently large. The electrical properties of carbon nanotube/polymer nanocomposites have also been studied using randomly distributed three-dimensional "soft-core" cylinders.[19] They calculated the NT-limited dc conductivity by transforming the percolating network to a three-dimensional (3D) resistor network. The ratio of the fiber length to the simulation cell size was assumed as 5.0. The critical exponent t was identified as 1.8 ± 0.05 independent of the aspect ratio. This value is consistent with the universal value of 2.0 in 3D case.[1]

Recently, however, it has been suggested experimentally that the universality does not hold for carbon nanofiber/polyimide nanocomposites.[20] As for the value of the critical exponent t, it has been pointed out that the value of t depends on both the range of the concentration and the transport mechanism, that is, the contact-resistance-limited or the nanotube-resistance-limited.[21] Furthermore, it has been shown that the percolation conductivity depends on alignment as well as concentration of nanotubes and both dependences exhibit the critical power-law behavior.[22] The vertical dc conductance has a remarkable maximum at a specific alignment. In the aligned case, strong anisotropy of the dc conductance has also been confirmed. The reason why the dc conductivity takes the remarkable maximum at a specific alignment has not been clarified yet.

Our aim is to investigate the complex ac admittance of a thin film of carbon nanotube/polymer composites and to reveal the dependences on both the concentration and the degree of alignment of nanotubes, taking into account the contact resistance between nanotubes. We calculate numerically both the complex ac admittance and the current intensity distribution by a transfer matrix method,[4,24] by transforming the discretized mesh model for a thin film of nanotube/polymer composites into the RC network. As for the dc conductivity, we study two extreme cases; the nanotube-resistance (NT)-limited case and the contact-resistance (CR)-limited case.

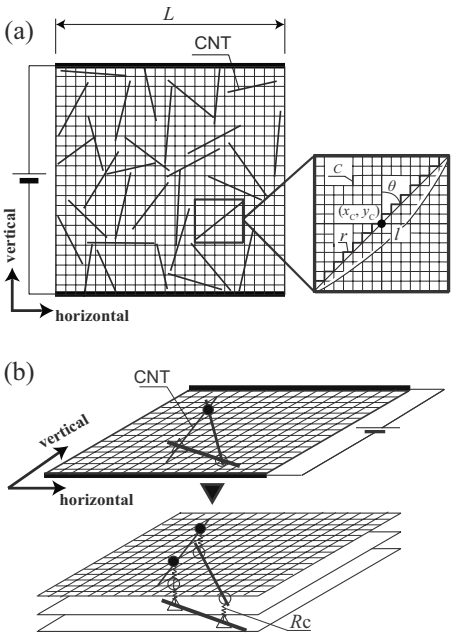

FIG. 1. (a) Schematic figure of a two-dimensional discretized mesh model for a stick model in a continuous two-dimensional area and its transformation to the RC network. (b) Extension of the 2D discretized mesh model into the multilayer model to consider the contact-resistance R_c between crossing nanotubes.

II. MODEL

We consider a 2D thin film of nanotube/polymer composites and calculate numerically both the complex ac admittance and the current intensity distribution using the 2D RC network in the discretized mesh model. In Fig. 1(a), we present schematically how a two-dimensional stick model for a thin film of nanotube/polymer composites is discretized by dividing the continuous area into a mesh and is transformed to the RC network. Here, we assume the length of a nanotube as l, the resistance between two ends of the nanotube as R and the capacitance per square of polymers as C. The discretized mesh model is transformed to the RC network, by assigning a resistor $r=R/N$ for each bond along a nanotube and a capacitor C for all the other bonds. Here, N is the total number of bonds along a nanotube and N depends on the alignment of each nanotube. The angle between the axis of a nanotube and the vertical axis is set as θ. The alignment of nanotubes is characterized by the cutoff angle θ_μ as θ is distributed uniformly within the cutoff angle.

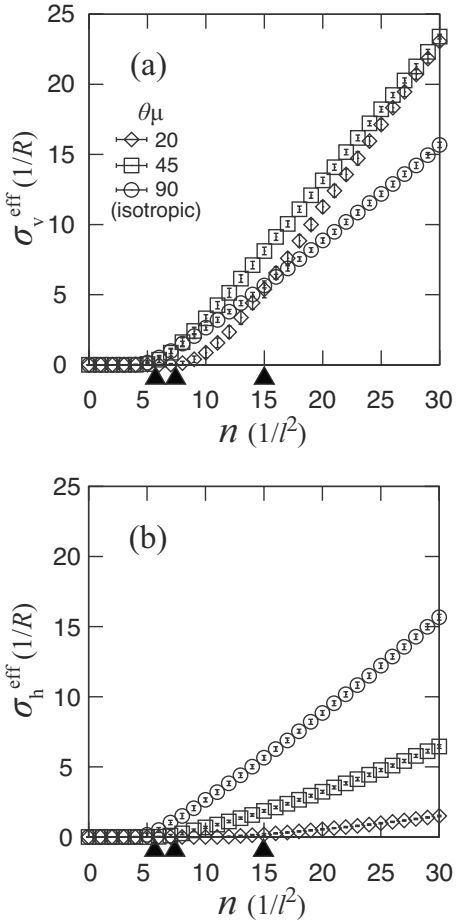

FIG. 2. Concentration dependence of (a) the vertical component σ_v^{eff} and (b) the horizontal component σ_h^{eff} of the effective conductance for three values of θ_μ. Here, three arrow- heads indicate the percolation thresholds calculated in a continuous stick model (Ref. 23) for each alignment and the percolation threshold increases with decrease of θ_μ.

$$-\theta_\mu \leq \theta \leq \theta_\mu. \tag{1}$$

We define the concentration n of nanotubes as the number of nanotubes per l^2. The center of nanotubes are distributed at random in a square of $L \times L$.

To consider the contact-resistance between nanotubes, we extended the two-dimensional *RC*-network into the multilayered *RC* network as shown in Fig. 1(b). Here, we take the contact resistance between nanotubes as R_c and all the other connections between layers are assumed to have an infinite resistance. In the superimposed layers, a resistor $r=R/N$ is assigned for each bond along the nanotube but all the other lateral bonds within the layer are assumed to have an infinite resistance.

We apply a transfer matrix method to calculate both the complex ac admittance tensor Y and the current distribution for the *RC* network.[4,24] We can easily take into account the effect of the displacement current through polymer in the discretized mesh model. The transfer matrix method is appropriate to treat the large lattice using the recursion formula. In our computation, we avoided a lot of calculations of matrix inversions which appear in the original formula,[4] by adding the resistor or the capacitor one by one to the *RC* network. From the complex admittance tensor Y, the effective conductance tensor σ^{eff} and the effective capacitance tensor C^{eff} can be derived as,

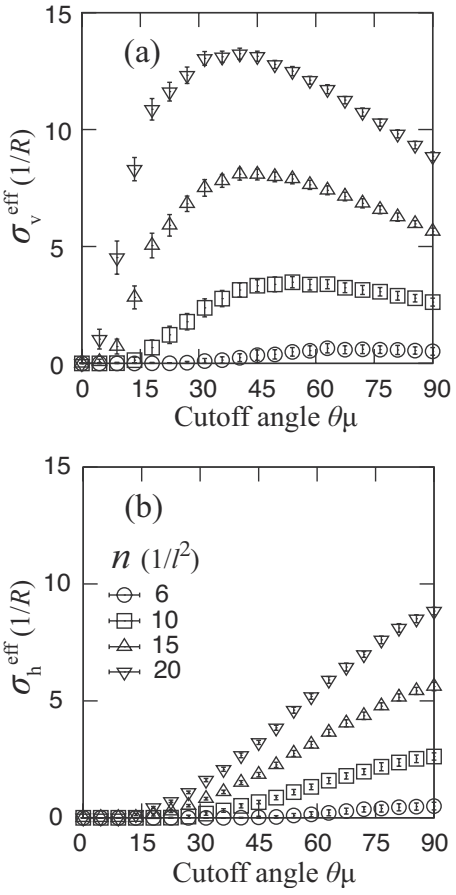

FIG. 3. The alignment dependence of (a) the vertical component σ_v^{eff} and (b) the horizontal component σ_h^{eff} of the effective conductance for four values of the nanotube concentration, n.

$$Y = \sigma^{eff} + i\omega C^{eff}, \tag{2}$$

where ω is the angular frequency of ac current. Each element of the complex admittance can also be written as $Y = |Y|\exp(i\Phi)$ and the dielectric loss can be calculated from the dielectric constant ε (C) as Im ε/Re $\varepsilon = 1/\tan\Phi$. In our calculations, we assumed a constant dielectric constant for the polymer and the effective capacitance C^{eff} has a constant value at low frequencies.

In the numerical calculation, we assume the system size of $L=10l$ and the mesh size of $\Delta=l/20$. We checked a finite mesh-size effect on the dc conductivity in the isotropic case for $L=10l$ at three NT concentrations, $nl^2=6$, 7 and 10. The finite mesh-size effect becomes more remarkable as NT concentration decreases and approaches the percolation threshold, and it always overestimates the conductivity. The effect is significant at $\Delta=l/10$ but it is greatly suppressed at $\Delta=l/20$ and becomes negligible at $\Delta=l/30$. Computation at $\Delta=l/30$ was desirable but required a long CPU time, thus we adopted a mesh size of $\Delta=l/20$. We checked also a finite

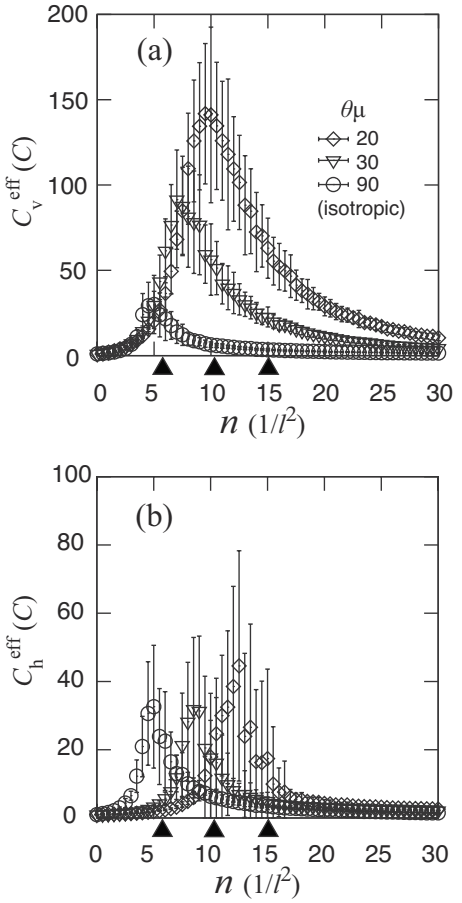

FIG. 4. Concentration dependence of (a) the vertical component C_v^{eff} and (b) the horizontal component C_h^{eff} of the effective capacitance for three values of θ_μ, with the percolation threshold (Ref. 23) indicated by arrow-heads.

cell-size effect on the dc conductivity at $\Delta = l/20$ for three NT concentrations, $nl^2 = 6$, 10 and 15. The finite cell-size effect also overestimates the conductivity, and its effect increases as the NT concentration approaches the percolation threshold. We adopted $L = 10l$, because the calculated conductivity at $L = 10l$ agrees with those at $L = 20l$ and $30l$ within an accuracy of 10% for $nl^2 = 6$. All the data are obtained by taking the ensemble average over 100 samples. We set the unit of the effective conductance σ^{eff} as $1/R$ or $1/R_c$ for the nanotube-resistance-limited or the contact-resistance-limited cases, respectively, and that of the effective capacitance as C. We set also the unit of the angular frequency ω as $1/RC$.

III. NUMERICAL RESULTS

First, we show in Fig. 2 the concentration dependence of the dc conductance for three typical alignments of nanotubes in the nanotube-resistance-limited case. It is seen that the vertical dc conductance becomes larger than the horizontal dc conductance with alignment of nanotubes. The percolation threshold[23] calculated in a continuous stick model[7,16,25,26] is also indicated by an arrow head for each alignment in Fig. 2 and the percolation threshold increases with decreasing θ_μ. These calculated percolation thresholds

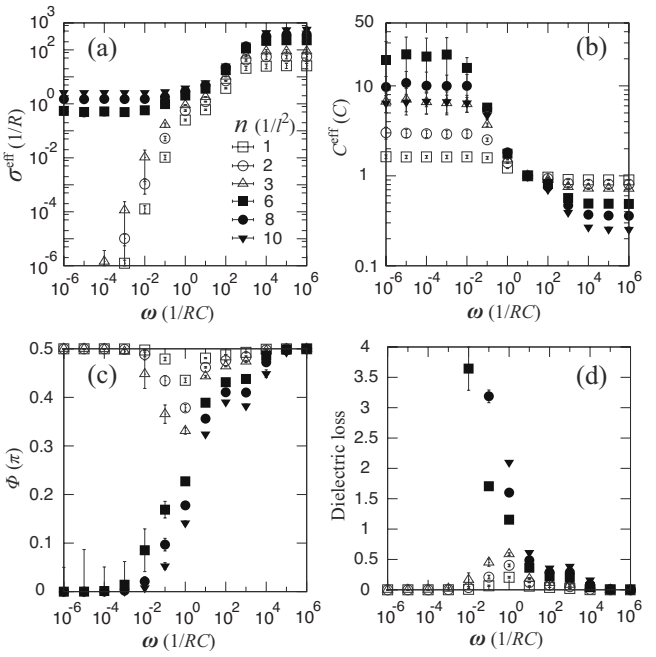

FIG. 5. (a) The effective conductance σ^{eff}, (b) the effective capacitance C^{eff}, (c) the argument of the complex admittance Φ^{eff}, and (d) the dielectric loss, Im ε^{eff}/Re $\varepsilon^{eff} = 1/\tan \Phi^{eff}$ vs angular frequency ω, for various nanotube concentrations in the isotropic case.

correspond well to the threshold of the horizontal dc conductance in Fig. 2(b), but the percolation threshold is much larger than the threshold of the vertical current at $\theta_\mu = 20°$ in Fig. 2(a). This large deviation in the aligned case is caused by a finite mesh-size effect and the effect becomes larger as θ_μ decreases. Recently, very accurate evaluation of the percolation threshold has been performed with a finite-size scaling method for the isotropic stick percolation.[27] In comparison to the result,[27] the calculated percolation threshold[23] has an accuracy within 2%. In Fig. 3, we show the alignment dependence of the dc conductance at fixed concentrations. The horizontal dc conductance increases monotonically with θ_μ, but the vertical dc conductance has a maximum at a specific alignment $\theta\mu^{max}$ and $\theta\mu^{max}$ decreases as the concentration, n, increases. The calculated behavior of the vertical conductance is consistent to the experimental result.[22]

Second, we present in Fig. 4 the concentration dependence of the effective capacitance (dielectric constant) for three alignments in the nanotube-resistance-limited case. The effective capacitance is remarkably enhanced near the percolation threshold as observed by experiment.[13,14] The enhancement of the vertical component is much larger than that of the horizontal one in the aligned case and the enhancement of the vertical capacitance is further enlarged as θ_μ decreases as seen in Fig. 4(a). Hence, the vertical effective capacitance becomes much larger than the horizontal effective capacitance for the aligned case. The deviation of the concentration at the maximum of the capacitance from the percolation threshold is due to the finite mesh-size effect as mentioned before.

Third, we show in Fig. 5 the frequency dependence of the effective conductance, the effective capacitance, the argument of the complex admittance, and the dielectric loss in the

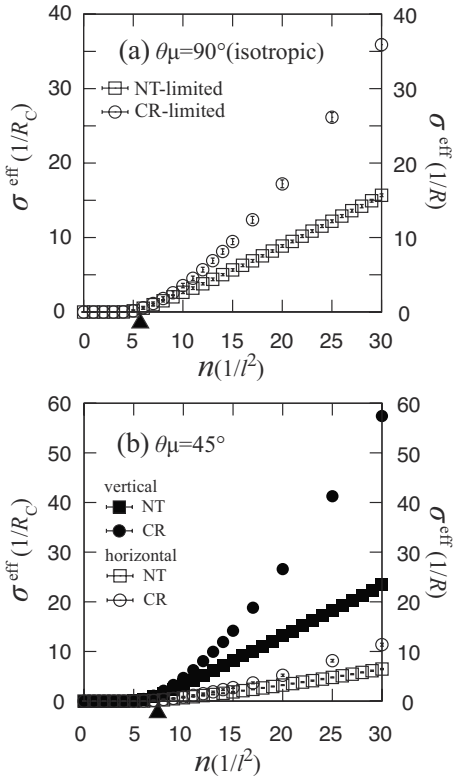

FIG. 6. Comparison between the concentration dependence of the nanotube- resistance-limited conductance and the contact-resistance-limited conductance in (a) the isotropic case of $\theta_\mu=90°$ and (b) the aligned case of $\theta_\mu=45°$, respectively. In the aligned case, both the vertical and the horizontal conductances are plotted. The arrow head indicates the percolation threshold calculated in a continuous stick model (Ref. 23).

isotropic case. The effective conductance is constant at low frequencies and increases monotonically at high frequencies for metallic concentrations, although it decreases to zero with decreasing frequency in the insulating region. On the other hand, the effective capacitance decreases monotonically with the frequency for both metallic and insulating regions, and they have constant values at high frequencies. Corresponding to these behaviors, the argument of the complex admittance increases monotonically from 0 to $\pi/2$ in the metallic concentration, while in the insulating region it has a value of $\pi/2$ in both low and high frequencies except the frequency region around $\omega RC=1$. Hence, the dielectric loss decreases monotonically in the metallic concentration, although it exhibits a small peak around $\omega RC=1$ in the insulating region. This behavior of the dielectric loss in the insulating region agrees with the observed result.[13]

Finally, we calculate the dc conductance of the CR-limited case and compare it with that of the NT-resistance-limited case; the results are shown in Fig. 6 In both the isotropic and the aligned cases, the CR-limited conductance has a stronger concentration dependence in the range above about $2n_c$, while they have similar dependence to the NT-limited conductance in the range below about $2n_c$. In the aligned case in Fig. 6(b), both the vertical and the horizontal conductances are plotted. To study the alignment dependence of the CR-limited conductance, we plot in Fig. 7 the vertical

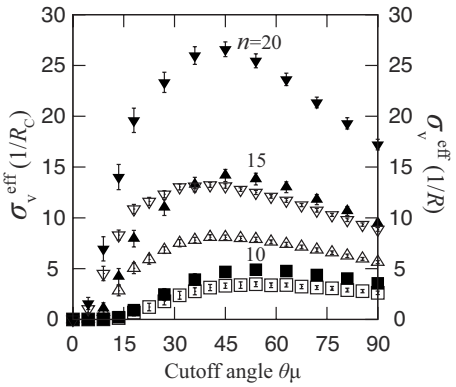

FIG. 7. The alignment dependence of the vertical CR-limited conductance σ_v^{eff} (solid squares, solid triangles, and solid inverse triangles) at three values of the nanotube concentration, $n=10$, 15, and 20, respectively, with those of the vertical NT-limited conductance (open squares, open triangles, and open inverse triangles).

CR-limited conductance as a function of the cutoff angle θ_μ, with the NT-limited vertical conductance. The vertical CR-limited conductance has a steeper decrease above the peak cutoff angle than the NT-limited conductance, especially in higher NT concentrations.

IV. DISCUSSION AND CONCLUSION

First, we discuss the reason why the vertical dc conductance has the maximum at a specific alignment. To reveal the

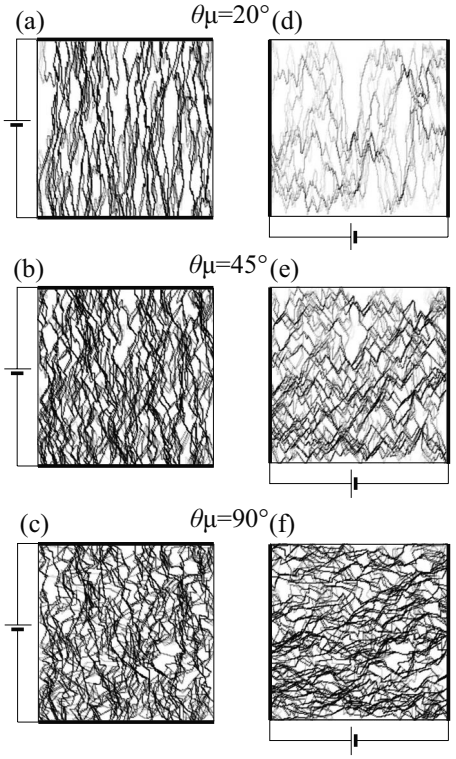

FIG. 8. Intensity distribution at $n=15$ of the vertical dc current for the alignment of (a) $\theta_\mu=20°$, (b) $\theta_\mu=45°$, (c) $\theta_\mu=90°$, and that of the horizontal dc current for the alignment of (d) $\theta_\mu=20°$, (e) $\theta_\mu=45°$, and (f) $\theta_\mu=90°$, respectively.

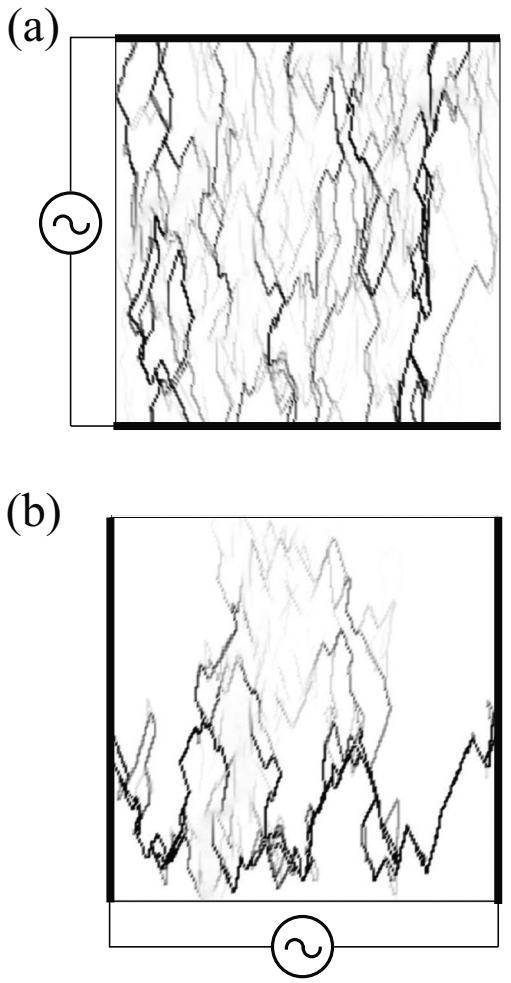

FIG. 9. Intensity distribution of the imaginary current in (a) the vertical direction and (b) the horizontal direction, respectively. Here $n=7$ and $\theta_\mu=30°$.

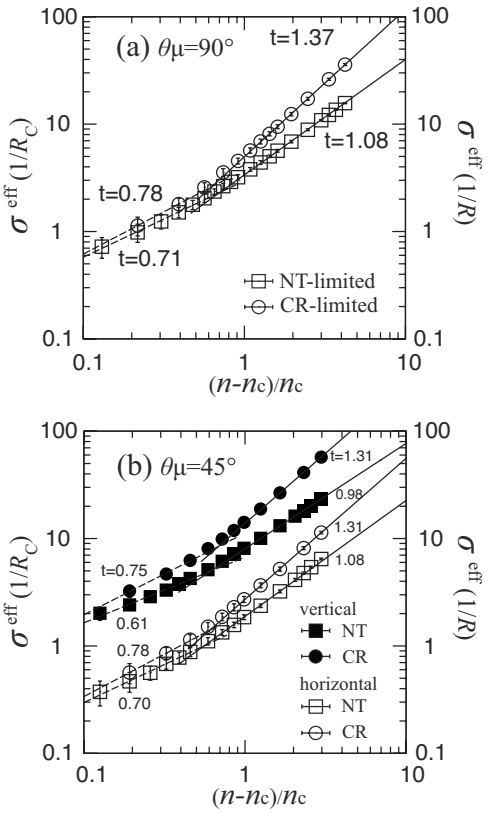

FIG. 10. Comparison between the concentration dependence of the nanotube limited conductance and the contact-resistance-limited conductance in (a) the isotropic case of $\theta_\mu=90°$ and (b) the aligned case of $\theta_\mu=45°$, respectively, in the log-log plot. In the aligned case, both the vertical and the horizontal conductances are plotted. The best fitted power-law relations are also plotted with a broken line near the percolation threshold and a solid line in a higher concentration range.

origin, we calculate the intensity distribution of the vertical current at $n=15$ for three alignments in Figs. 8(a)–8(c). The dc conductance has the maximum around $\theta_\mu=45°$ as seen in Fig. 3 and the number of current paths decreases as θ_μ decreases from 45°. As clearly seen in Figs. 8(a)–8(c), the degree of meandering increases as θ_μ increases from 45°. Hence, the dc conductance has the maximum around 45° at $n=15$. On the other hand, the horizontal dc conductance increases monotonically as θ_μ increases as shown in Fig. 3, and it is smaller than the vertical dc conductance in the aligned case. The intensity distribution of the horizontal current is also presented in Figs. 8(d)–8(f). As θ_μ increases, the number of current paths increases and the degree of meandering is also suppressed. Hence, the horizontal dc conductance increases monotonically with θ_μ.

Next, in order to consider the reason why the enhancement of the vertical effective capacitance near the percolation threshold is enlarged by the alignment of nanotubes, we calculate the intensity distribution of both the vertical and the horizontal imaginary current at $\theta_\mu=30°$ in Fig. 9. A part of the kink point in the current path corresponds to a mini-gap between nanotubes. The number of current paths is larger and the number of serial connections of a minigap capacitors along each current path is smaller for the vertical imaginary current than for the horizontal imaginary current. This means the number of parallel connections of capacitors is larger and the number of serial connections of the minigap capacitors is smaller for the vertical imaginary current compared to the horizontal current. Hence, the vertical effective capacitance is much larger than the horizontal effective capacitance. Furthermore, the number of the serial connections of minigap capacitors decreases and the number of the parallel current paths increases by decreasing θ_μ. This is the origin of enlarged vertical effective capacitance by alignment of nanotubes.

Third, we discuss the frequency dependence of the complex admittance. The most remarkable feature of nanotube/polymer composites is that the argument Φ of the complex admittance in the metallic region increases in a monotonic way from 0 to $\pi/2$, contrary to the random lattice system[28,29] where Φ in the metallic region approaches to 0 in both low and high frequencies. This means that the imaginary current through capacitors becomes more dominant at higher frequencies in comparison to the real current through nanotubes.

Finally, we discuss the difference between the concentration dependences of the nanotube-resistance-limited conduc-

tance and the contact-resistance-limited conductance. To estimate the critical exponent, we plot the dc conductance in the log-log plot in Fig. 10. It is seen from Fig. 10 that the critical exponent t has the same value independent of the degree of alignment of nanotubes within the "experimental" uncertainty. Furthermore, the critical exponents have the same value for the vertical conductance and the horizontal conductance in the aligned case. However, it clearly depends on the resistivity mechanism, the NT-limited or the CR-limited, contrary to the result by Balberg.[16] In the concentration region higher than about $2n_c$, the CR-limited dc conductance has a concentration dependence with the critical exponent of $t \approx 1.3$ in agreement with the universal value of $t=1.3$ in 2D case.[3] However, the NT-limited conductance has a smaller exponent of $t \approx 1.0$. The reason for this difference is considered to be similar root to that pointed out by Keblinski *et al.*[21] If we double the intersecting two fibers in parallel connection as all the four fibers intersect with each other, the CR-limited conductivity quadruples while the NT-limited conductivity doubles. This suggests that $\sigma \propto n$ for the NT-limited conductance and $\sigma \propto n^2$ for the CR-limited conductance. Indeed, the NT-limited conductance with $t \approx 1.0$ in Fig. 10 agrees well with this picture, but the CR-limited result in Fig. 10 has a much smaller value of $t \approx 1.3$ in comparison with 2. The exponent t has a smaller value in the low concentration less than about $2n_c$. We cannot discuss this concentration region at present, because both the finite mesh-size effect and the finite cell-size effect cannot be neglected in the vicinity of the percolation threshold.

In summary, we study the complex ac admittance of carbon nanotube/polymer composites and reveal the dependences on both the concentration and the degree of alignment of nanotubes. We calculate numerically both the complex admittance and the current intensity distribution on the basis of the 2D discretized mesh model, by applying a transfer matrix method to the *RC* network. The percolation threshold increases with the alignment of nanotubes. The vertical dc conductivity parallel to the alignment direction has a maximum at a specific alignment, caused by competition between the number of percolating paths and the degree of meandering of the current path. As for the concentration dependence of the dc conductivity, we study two extreme cases, namely, the nanotube-resistance (NT)-limited case and the contact-resistance (CR)-limited case. CR-limited conductivity has the critical exponent of $t \approx 1.3$, which is in agreement with the universal value, and exhibits a little stronger concentration dependence than NT-limited conductivity above $2n_c$, because the practical number of the parallel connection of resistors becomes larger for CR-limited conductivity. The vertical static dielectric constant is enhanced near the percolation threshold and the enhancement is enlarged by alignment of nanotubes, caused by both decrease of the number of the serial connections of minigap capacitors and the increase of the number of parallel paths of the imaginary current.

In a following paper,[23] we reveal the dependence of the percolation threshold on the alignment of nanotubes on the basis of a continuous stick model. We use the continuous model to reduce both effects of a finite mesh size in the discretized mesh model and a finite cell size with a finite ratio of the nanotube length to the simulation cell size. Furthermore, we present the geometric critical exponent β and show that the universality does not hold for nanotube/polymer composites in 2D case.

ACKNOWLEDGMENTS

We acknowledge Shigeru Kohinata in Sumitomo Metal Mining Co. for stimulating discussion on high frequency conductance on conductive epoxy adhesive. This is a trigger for this work.

*junj@ee.uec.ac.jp

[1] D. J. Bergman, Solid State Phys. **46**, 147 (1992).
[2] A. L. Efros and B. I. Shklovskii, Phys. Status Solidi **76**, 475 (1976).
[3] D. J. Bergman and Y. Imry, Phys. Rev. Lett. **39**, 1222 (1977).
[4] B. Derrida and J. Vannimenus, J. Phys. A **15**, L557 (1982).
[5] D. Wilkinson, J. S. Langer, and P. N. Sen, Phys. Rev. B **28**, 1081 (1983).
[6] M. E. J. Newman and R. M. Ziff, Phys. Rev. Lett. **85**, 4104 (2000).
[7] I. Balberg, C. H. Anderson, S. Alexander, and N. Wagner, Phys. Rev. B **30**, 3933 (1984).
[8] R. Ramasubramaniam, J. Chen, and H. Liu, Appl. Phys. Lett. **83**, 2928 (2003).
[9] B. Kim, J. Lee, and I. Yu, J. Appl. Phys. **94**, 6724 (2003).
[10] M. Grujicic, G. Cao, and W. N. Roy, J. Mater. Sci. **39**, 4441 (2004).
[11] M. Foygel, R. D. Morris, D. Anez, S. French, and V. L. Sobolev, Phys. Rev. B **71**, 104201 (2005).
[12] B. E. Kilbride, J. N. Coleman, J. Fraysse, P. Fournet, M. Cadek, A. Drury, S. Hutzler, S. Roth, and W. J. Blau, J. Appl. Phys. **92**, 4024 (2002).
[13] L. Wang and Z. Dang, Appl. Phys. Lett. **87**, 042903 (2005).
[14] M. Jiang, Z. Dang, and H. Xu, Appl. Phys. Lett. **90**, 042914 (2007).
[15] G. D. Liang and S. C. Tjong, IEEE Trans. Dielectr. Electr. Insul. **15**, 214 (2008).
[16] I. Balberg, N. Binenbaum, and C. H. Anderson, Phys. Rev. Lett. **51**, 1605 (1983).
[17] H. Gould and J. Tobochnik, *An Introduction to Computer Simulation Methods: Applications to Physical Systems* (Addison-Wesley, Reading, 1988).
[18] T. Zhang and Y. B. Yi, J. Appl. Phys. **103**, 014910 (2008).
[19] N. Hu, Z. Masuda, C. Yan, G. Yamamoto, H. Fukunaga, and T. Hashida, Nanotechnology **19**, 215701 (2008).
[20] A. Trionfi, D. H. Wang, J. D. Jacobs, L. S. Tan, R. A. Vaia, and J. W. P. Hsu, Phys. Rev. Lett. **102**, 116601 (2009).
[21] P. Keblinski and F. Cleri, Phys. Rev. B **69**, 184201 (2004).
[22] F. Du, J. E. Fischer, and K. I. Winey, Phys. Rev. B **72**,

121404(R) (2005).
[23] N. Ainoya, Y. Hazama, J. Nakamura, and A. Natori (unpublished).
[24] D. J. Bergman, E. Duering, and M. Murat, J. Stat. Phys. **58**, 1 (1990).
[25] G. E. Pike and C. H. Seager, Phys. Rev. B **10**, 1421 (1974).
[26] I. Balberg and N. Binenbaum, Phys. Rev. B **28**, 3799 (1983).
[27] J. Li and S.-L. Zhang, Phys. Rev. E **80**, 040104(R) (2009).
[28] T. B. Murtanto, S. Natori, J. Nakamura, and A. Natori, Phys. Rev. B **74**, 115206 (2006).
[29] Y. Hazama, J. Nakamura, and A. Natori, J. Mater. Sci. **45**, 2843 (2010).